Mon. Not. R. Astron. Soc. **000**, 000–000 (0000) Printed 2 February 2008

The fundamental plane of isolated early-type galaxies

Fatma M. Reda,[1,2⋆] Duncan A. Forbes[1⋆] and George K.T. Hau[3⋆]
[1] *Centre for Astrophysics & Supercomputing, Swinburne University, Hawthorn, VIC 3122, Australia*
[2] *Astronomy Department, National Research Institute of Astronomy and Geophysics, Helwan, Cairo 11421, Egypt*
[3] *Department of Physics, South Road, Durham, DH1 3LE, U.K.*

arXiv:astro-ph/0505265v1 12 May 2005

2 February 2008

ABSTRACT

Here we present new measurements of effective radii, surface brightnesses and internal velocity dispersions for 23 isolated early-type galaxies. The photometric properties are derived from new multi-colour imaging of 10 galaxies, whereas the central kinematics for 7 galaxies are taken from forthcoming work by Hau & Forbes. These are supplemented with data from the literature. We reproduce the colour-magnitude and Kormendy relations and strengthen the result of Paper I that isolated galaxies follow the same photometric relations as galaxies in high density environments. We also find that some isolated galaxies reveal fine structure indicative of a recent merger while others appear undisturbed. We examine the Fundamental Plane in both traditional R_e, μ_e and σ space and also κ-space. Most isolated galaxies follow the same Fundamental Plane tilt and scatter for galaxies in high density environments. However, a few galaxies notably deviate from the plane in the sense of having smaller M/L ratios. This can be understood in terms of their younger stellar populations, which are presumably induced by a gaseous merger. Overall, isolated galaxies have similar properties to those in groups and clusters with a slight enhancement in the frequency of recent mergers/interactions.

Key words: galaxies: elliptical and lenticular, cD - galaxies: formation - galaxies: fundamental parameters - galaxies: photometry - galaxies: structure.

1 INTRODUCTION

The observational studies of Djorgovski & Davis (1987) and Dressler (1987) found that elliptical galaxies are confined to a tight plane defined by: $R_e \propto \sigma^{\alpha} < \mu_e >^{\beta}$ in the 3 dimensional space of central velocity dispersion (σ), effective radius (R_e) and mean surface brightness ($< \mu_e >$) enclosed by R_e, where α and β are coefficients. This plane is known as the Fundamental Plane (FP), and it has a small intrinsic scatter in its edge-on projection suggesting a strong regularity in the process of elliptical galaxy formation (Jørgensen, Franx & Kjærgaard 1993; JFK93).

Theoretically, the FP can be derived from the scalar form of the virial theorem as: $R_e = K_s\ \sigma^2\ < \mu_e >^{-1}\ (M/L)^{-1}$, where K_s is a structure parameter which depends on the luminosity, kinematic and density structure of a galaxy, and (M/L) is the mass-to-light ratio (Djorgovski, de Carvalho & Han 1988). The observed and theoretical forms of the FP are identical only if the term $K_s\ (M/L)^{-1}$ is a power-law function of σ and/or $< \mu_e >$. The observed intrinsic scatter of the FP implies a deviation of the relation from the pure power-law form. These deviations reflect the effects of galaxy formation and evolutionary processes. Assuming that early-type galaxies are homologous, i.e. have similar kinematic, luminosity, and density distributions so that K_s = constant, then the FP reflects the evolution of the M/L ratio, i.e. their stellar population and dark matter content. However, a combination of stellar population and non-homology dependence of the FP tilt is also plausible (Trujillo, Burkert & Bell 2004).

Various theoretical studies have attempted to reproduce the FP in terms of the merger and/or collapse history of galaxies, and its subsequent effects on star formation (e.g. Hjorth & Madsen 1995; Capelato, de Carvalho & Carlberg 1995; Levine 1997; Bekki 1998; Dantas et al. 2003; Nipoti, Londrillo & Ciotti 2003). In a hierarchical universe, galaxies in low-density regions are the last to collapse and should thus be younger than galaxies which collapsed early in the higher density regions (e.g. Kauffmann et al. 2004).

The effect of local environment on a galaxy's formation history and fundamental parameters has been the motivation for many studies. Environmental effects have been seen in galaxy scaling relations. For example, in a comparison study of early-type galaxies in the field, groups and

⋆ E-mail: freda@astro.swin.edu.eu (FMR); dforbes@swin.edu.au (DAF); george.hau@durham.ac.uk (GKTH)

rich clusters, de Carvalho & Djorgovski (1992) found that field galaxies showed more intrinsic scatter in their properties than those in clusters, especially when stellar population variables were included. In a study of 9000 early-type galaxies from the Sloan Digital Sky Survey, Bernardi et al. (2003b) found that the scatter from the FP correlates weakly with the galaxy local environment. These variations are in the sense that galaxies in dense regions are slightly fainter, or have higher velocity dispersions, than in less dense regions (Bernardi et al. 2003a). The results of both de Carvalho & Djorgovski (1992) and Bernardi et al. (2003b) suggest a more extended formation epoch for galaxies in the field versus those in clusters. This is supported by studies that measure the luminosity-weighted age of galaxies in different environments (e.g. Terlevich & Forbes 2002; Proctor et al. 2004). Interestingly, Evstigneeva, Reshetnikov & Sotnikova (2002) have reported no significant difference in the tilt and scatter of the Fundamental Plane for strongly interacting early-type galaxies.

Previous studies of the FP in different environments have not been extended to the very low densities of truly isolated galaxies. In such extreme low-density environments we can eliminate the effect of many physical processes, such as tidal interactions, ram-pressure stripping, strangulation, high-speed galaxy-galaxy interactions and ongoing mergers, all of which may affect the evolution of galaxies in denser environments.

Here, we further study the sample of 36 early-type isolated galaxies introduced in Reda et al. (2004; Paper I). We present imaging in the B and R-bands for another 10 galaxies in the sample. These images are used to study the internal morphological structure of these 10 galaxies and to obtain their magnitudes and colours. The main aspect of this work however is to investigate the FP for isolated galaxies and compare it with that for galaxies in higher density environments. Our photometric parameters are supplemented by kinematic data from Hau & Forbes (inpreparation, hereafter HF05) and from the literature. Based on the results of this study, we briefly discuss the implications for the formation of isolated early-type galaxies.

2 PHOTOMETRIC PARAMETERS

2.1 Observations and data reduction

In this paper we present imaging in the B and R-bands for 10 galaxies in our sample (the original sample of 36 isolated galaxies was introduced in Paper I). Images were obtained using the Wide Field Imager (WFI) on the ESO/MPG 2.2-m telescope on 2001 August 7-10. Each galaxy had many exposures which were combined to give an average integration time as summarized in Table 1. The median seeing conditions over the three nights were $1.3''$ in B and $1.1''$ in the R-band. Observations of standard star fields from Landolt (1992) were obtained during the three nights. All galaxy and standard star fields were reduced using the ESOWFI package within IRAF.

Table 1. Photometric measurements.

Galaxy	Filter	Magnitude (mag)	Exp.time (sec)
NGC 6653	B	12.8 ± 0.1	120
	R	11.4 ± 0.1	120
NGC 6776	B	12.5 ± 0.1	180
	R	10.9 ± 0.1	300
NGC 6799	B	13.3 ± 0.1	120
	R	11.8 ± 0.1	120
NGC 6849	B	12.9 ± 0.1	120
	R	11.6 ± 0.1	120
NGC 7796	B	12.2 ± 0.1	120
	R	10.6 ± 0.1	120
MCG-01-03-018	B	13.4 ± 0.1	180
	R	12.0 ± 0.1	120
ESO107-G004	B	12.6 ± 0.2	120
	R	11.2 ± 0.2	120
ESO153-G003	B	13.7 ± 0.1	120
	R	12.1 ± 0.1	120
ESO194-G021	B	13.3 ± 0.1	120
	R	11.6 ± 0.1	120
ESO462-G015	B	12.5 ± 0.2	120
	R	11.0 ± 0.1	120

Notes: Measured magnitudes and total exposure time in B and R-bands for the galaxies observed on the ESO/MPG 2.2-m telescope.

2.2 Magnitudes, surface brightnesses and effective radii

To obtain the photometric parameters of these galaxies, we followed the same technique as in Paper I and corrected them for Galactic extinction using values from Schlegel, Finkbeiner & Davis (1998). The QPHOT task in IRAF was used to obtain aperture magnitudes of each galaxy and compute the sky level in an annulus of 1000 pixels and width of 50 pixels. Then, the total magnitudes (Table 1) were derived by fitting a curve-of-growth to the galaxy aperture magnitudes. To obtain the absolute magnitudes (M_B) listed in Table 2, we used the distances quoted in Paper I.

Again following the same technique as in Paper I, the ISOPHOTE package in IRAF was used to fit a smooth elliptical model to the galaxy image. During the modelling process, the galaxy centre, position angle and ellipticity were allowed to vary. The surface brightness profile of the galaxies were fit to a de Vaucouleurs $R^{1/4}$ law, from which we obtained the effective radius (R_e) and the mean effective surface brightness ($< \mu_e >$). The error estimate for R_e and $< \mu_e >$ was based on the variation during the fitting procedure.

2.3 Other sources of the photometric parameters

In Paper I, we obtained R_e and $< \mu_e >$ for 8 galaxies of our sample. These observations were obtained in the B and R filters using the Wide Field Imager (WFI) on the 3.9-m Anglo-Australian Telescope (AAT). For details of the data reduction and the derived photometric parameters see Paper I.

Additional data are taken from the photometric catalogue by Prugniel & Heraudeau (1998; PH98) which includes total B magnitudes and mean effective surface brightnesses $< \mu_e >_B$ for 21 galaxies of our total sample. Prugniel & Her-

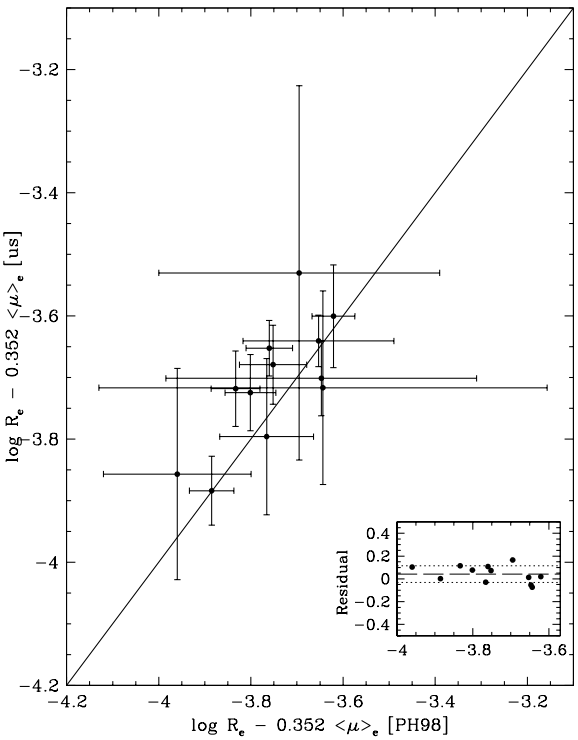

Figure 1. Comparison of our measurements of R_e and $< \mu_e >_B$ and those of Prugniel & Heraudeau (1998; PH98), using the edge-on projection of the Fundamental Plane from Jørgensen, Franx & Kjærgaard (1993). The solid line is the one-to-one relation. The inset shows the distribution of the residuals of our measurements from the one-to-one relation. The long-dashed line is the mean value of the residuals and the dotted lines represent the 1σ dispersion. The common measurements are consistent within the errors.

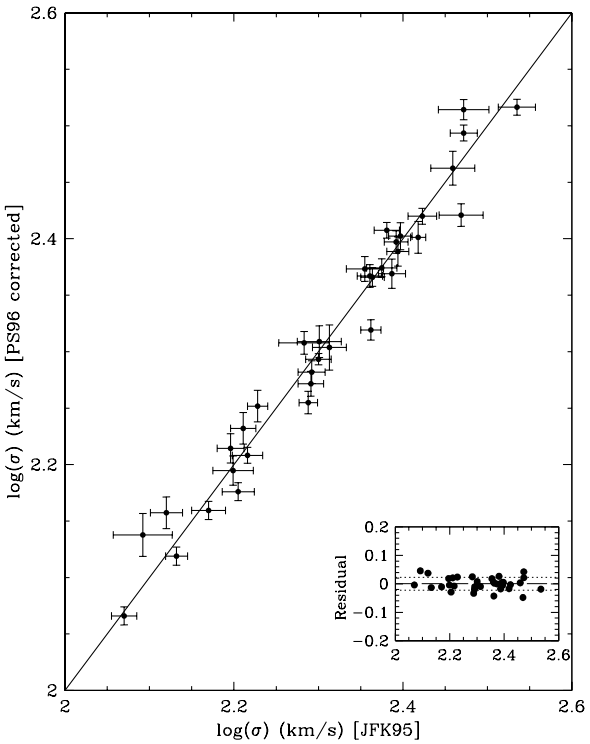

Figure 2. Comparison between the velocity dispersion values of 35 galaxies from Prugniel & Simien (1996; PS96) and values from Jørgensen, Franx & Kjærgaard (1995; JFK95) after applying the transformation $\sigma_{JFK95} = -0.11 + 1.04 \times \sigma_{PS96}$. The solid line is the one-to-one relation. The inset shows the distribution of the residuals as in Fig. 1. Good agreement is seen.

audeau fit their data using a linear interpolation between the de Vaucouleurs ($R^{1/4}$) and exponential profiles. We calculate R_e for galaxies from PH98 using their B and $< \mu_e >_B$ values as: $\log R_e = (< \mu_e >_B - B - 5.885)/5$. To check any systematic differences between our measurements and PH98 for R_e and $< \mu_e >_B$, we have computed the quantity $\log R_e - 0.352 < \mu_e >_B$ for the 12 galaxies in common with our observations. This is the edge-on projection of the FP from JFK93. Fig. 1 shows this quantity for the 12 galaxies in common. The inset in Fig.1 shows the distribution of the residuals of our measurements from the one-to-one relation. Our measurements show a slight systematic offset of 0.04 with small scatter of $1\sigma = 0.07$ which indicates good agreement. The final photometric parameters used in the present study are summarized in Table 2.

3 KINEMATIC PARAMETERS

HF05 have conducted a detailed kinematical study for 9 galaxies of our 36 isolated early-type galaxies. The galaxies were observed for 2×1200 seconds at the ESO 3.6-m telescope on the La Silla Observatory, Chile using a long slit of $1.5''$ and Grism#8. The slit was positioned roughly along the major axes of the galaxies and the spectra were summed inside a rectangular aperture of size $1.5'' \times 5''$. The velocity dispersion (σ) measurements were normalised to a diameter of $3.4''$ for a galaxy at the distance of Coma using the method of Jørgensen, Franx & Kjærgaard (1995; JFK95). For full details, see HF05.

In a recent study, Denicoló et al. (2005a; D05a) measured σ for 8 early-type galaxies of our isolated sample. They used the same normalization technique of JFK95 as in HF05. The galaxies were observed at the 2.12-m telescope of *The Observatorio Astrofísico Guillermo Haro*, in Cananea, Mexico. On average, they have eight observations for each galaxy in their study. These repeated observations per galaxy, and the deviation from the mean value, give an error on the mean velocity dispersion quoted.

Another source of internal kinematics for our galaxy sample is Prugniel & Simien (1996; PS96). In this catalogue, Prugniel & Simien compiled central velocity dispersions of 1698 galaxies from 3147 measurements. To homogenise the data that they collected from different literature sources, they identified a set of galaxies that have measurements from three or more references with deviations of 20 km/s or less. Using this list of "standard" galaxies, a scale factor was determined for each source and used to scale the velocity dispersion measurements for that source. Then, σ values were computed as the mean of the re-scaled measured veloc-

Table 2. Photometric and spectroscopic properties of the sample.

Galaxy	M_B (mag)	$< \mu_e >_B$ (mag/sq.$''$)	$\pm$	$\log R_e$ (pc)	$\pm$	Photometry source	$\log(\sigma)$ (km/s)	$\pm$	σ source
NGC 0821	-20.5	21.6	0.03	3.70	0.03	PH98	2.326	0.062	D05a
NGC 1045	-20.9	20.8	0.10	3.66	0.10	Paper I	2.360	0.061	D05a
NGC 1132	-21.8	22.5	0.10	4.12	0.05	Paper I	2.375	0.051	D05a
NGC 2110	-20.0	20.7	0.10	3.59	0.02	Paper I	2.400	0.007	HF05
NGC 2271	-20.0	20.9	0.06	3.47	0.07	PH98	2.400	0.005	HF05
NGC 2865	-20.7	20.8	0.10	3.68	0.01	Paper I	2.250	0.004	HF05
NGC 3562*	-21.8	21.8	0.09	4.02	0.07	PH98	2.432	0.016	PS96
NGC 6172	-20.4	20.8	0.10	3.61	0.06	Paper I	2.130	0.038	D05a
NGC 6411*	-21.2	21.9	0.12	3.90	0.04	PH98	2.248	0.034	D05a
NGC 6653	-21.1	21.6	0.10	3.92	0.02	ESO	2.337	0.041	PS96
NGC 6702	-21.5	22.3	0.05	4.04	0.04	PH98	2.243	0.011	PS96
NGC 6776	-21.7	21.1	0.10	3.90	0.11	ESO	2.316	0.028	PS96
NGC 6799	-21.1	21.3	0.10	3.77	0.02	ESO	2.178	0.015	PS96
NGC 6849	-21.6	22.2	0.10	4.16	0.01	ESO	2.328	0.014	PS96
NGC 7796	-21.0	21.1	0.10	3.71	0.02	ESO	2.414	0.015	PS96
IC 1211*	-21.0	21.9	0.03	3.88	0.06	PH98	2.295	0.028	PS96
MCG-01-27-013	-21.4	22.0	0.10	3.98	0.05	Paper I	2.390	0.006	HF05
MCG-01-03-018	-21.0	22.3	0.10	3.96	0.01	ESO	2.281	0.031	D05a
MCG-03-26-030	-21.7	21.4	0.10	3.92	0.02	Paper I	2.500	0.005	HF05
ESO107-G004	-20.4	21.4	0.20	3.68	0.06	ESO	2.242	0.114	PS96
ESO218-G002	-20.9	21.5	0.10	3.76	0.11	Paper I	2.450	0.005	HF05
ESO318-G021	-20.7	21.7	0.04	3.77	0.01	PH98	2.390	0.003	HF05
ESO153-G003	-20.9	20.6	0.10	3.62	0.06	ESO	-	-	-
ESO194-G021	-19.7	21.0	0.10	3.47	0.02	ESO	-	-	-
ESO462-G015	-22.0	21.3	0.20	3.90	0.02	ESO	2.378	0.088	D05a

Notes: The adopted data for the Fundamental Plane study. The sources of the photometric parameters are Reda et al. (2004; Paper I), Prugniel & Heraudeau (1998; PH98) and images obtained using the WFI on the ESO/MPG 2.2-m telescope for galaxies listed in Table 1 (ESO). Sources for the velocity dispersion are Hau & Forbes (2005; HF05), Denicoló et al. (2005a; D05a) and Prugniel & Simien (1996; PS96). The two galaxies ESO153-G003 and ESO194-G021 do not have available velocity dispersions. The three galaxies marked with "*" do not have R magnitude in PH98 and are excluded from the colour-magnitude analysis.

ity dispersion, weighted by the inverse of the squared mean error for each source. Errors in the PS96 catalogue are 1σ rms from the mean value.

The σ values quoted in PS96 were not normalized to the aperture size as in HF05 and D05a. In JFK95, they applied the aperture normalization technique to 220 galaxies in a range of environments. Their sample has 35 galaxies in common (after excluding galaxies with low S/N ratio) with the sample of PS96. Using the σ measurements of these common galaxies from JFK95 (σ_{JFK95}) and PS96 (σ_{PS96}), we obtained the transformation: $\log \sigma_{JFK95} = -0.11 + 1.04 \times \log \sigma_{PS96}$, which is used to convert the σ values from PS96 to be consistent with those of HF05 and D05a. These 35 galaxies cover the redshift range from $cz \approx 750$ km/s to 6500 km/s, which encompasses the range for our isolated galaxy sample. Any redshift-dependent aperture effect on the σ values is less than the dispersion of $\pm$ 10 km/s about the one-to-one line shown in Fig. 2. The inset in Fig.2 shows the distribution of the residuals of the corrected PS96 measurements from the one-to-one relation. The mean value of the residuals show a slight systematic offset of 0.0003 from the one-to-one relation with small scatter of $1\sigma = 0.022$ which indicates good agreement.

The catalogue of PS96 contains velocity dispersions for 18 galaxies of our sample. For the common galaxies between PS96 and HF05 (5 galaxies) and D05a (4 galaxies), we use the values from HF05 and D05a. Fig. 3 shows a comparison between the σ values from HF05 and D05a with PS96 for the 8 galaxies in common. For the galaxy NGC 2271, we use the velocity dispersion from Koproline & Zeilinger (2000) who quote a similar value to HF05.

The most deviant galaxy in Fig. 3 is the galaxy ESO318-G021 which has a velocity dispersion from PS96 that is significantly smaller than that from HF05. We have examined the possible cause for this discrepancy and conclude it is largely due to a mismatch of the template standard star. In HF05, a best-fit to the spectrum of ESO318-G021 was achieved using a K4 giant star, however when a K1 or K2 giant was used the velocity dispersion quoted by PS96 was reproduced (albeit with a higher chi-squared value). The exclusion of lines that are affected by emission increases the derived velocity dispersion, but the main difference between PS96 and the HF05 is due to the choice of stellar template. In the subsequent analysis we adopt the HF05 velocity dispersion for ESO318-G021. Considering all 9 galaxies in Fig. 3, the inset shows a mean value of the residuals from the one-to-one line of 0.04 with a scatter of $1\sigma = 0.08$.

4 RESULTS

4.1 Colour-magnitude relation

In Paper I, using the absolute magnitude in the R-band (M_R) and the $(B-R)$ colour of 8 isolated galaxies, we

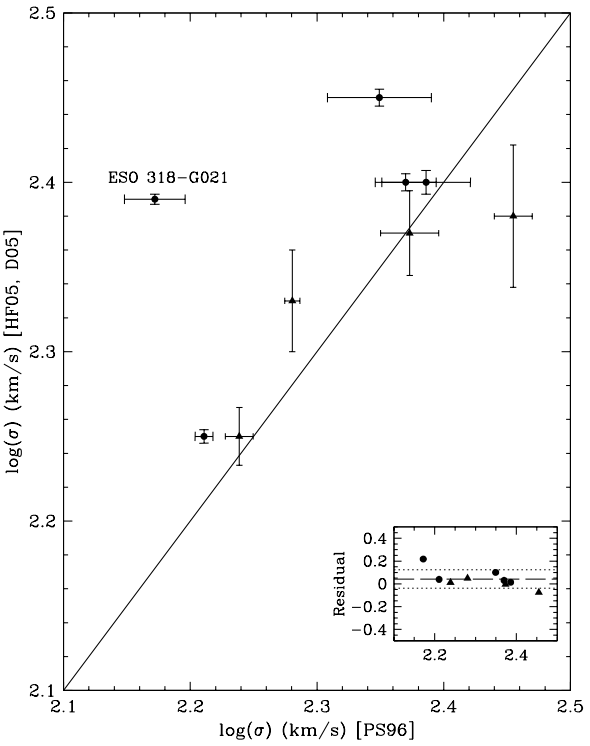

Figure 3. Comparison between the velocity dispersion values from Hau & Forbes (in preparation, hereafter HF05) shown as solid circles and Denicoló et al. (2005a; D05a) shown as solid triangles with those of Prugniel & Simien (1996; PS96). For NGC 2271 we use the value quoted in Koproline & Zeilinger (2000). The solid line is the one-to-one relation. The inset shows the distribution of the residuals as in Fig. 1. Reasonable agreement is seen, except for ESO318-G021 (see text for details).

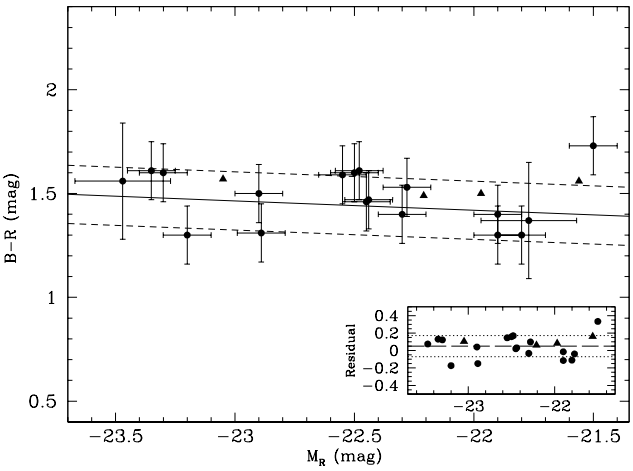

Figure 4. Colour-magnitude relation for the sample galaxies. The solid line (Gladders et al. 1998) represents the CMR of elliptical galaxies in the Coma cluster, while the short-dashed line indicates the mean error in the colour measurements for our sample galaxies. Solid circles are galaxies observed at the AAT (Paper I) and ESO/MPG 2.2-m telescope (this work), while solid triangles are galaxies from PH98 (error bars are not shown). The inset shows the distribution of the residuals as in Fig. 1. The isolated galaxies are consistent with the Coma cluster CMR.

showed that they follow a colour-magnitude relation (CMR) of slope and intrinsic scatter similar to that of early-type galaxies in the denser environment of the Coma cluster. In Fig. 4 we reproduce the CMR from Paper I and include the magnitudes and colours of the other 10 galaxies observed with the ESO/MPG 2.2-m telescope (Section 2.2). We also include 4 galaxies which have available colours from PH98. While the two galaxies ESO153-G003 and ESO194-G021 do not have published velocity dispersion in the literature, and are excluded from the FP analysis, they have available $(B-R)$ colour (Table 1) and are included in the CMR analysis. The three galaxies NGC 3562, NGC 6411 and IC 1211 do not have R magnitudes available in PH98 and are not considered in the CMR study (see Table 2). The residuals of our isolated galaxies from the CMR of galaxies in Coma cluster show a mean value of 0.05 with 1σ dispersion of 0.12 (see the inset in Fig. 4). Fig. 4 confirms our previous result of Paper I that isolated galaxies follow the CMR for galaxies in dense environments.

4.2 Internal fine structure

Using the same technique as Paper I, we have modelled each of the 10 galaxies observed at ESO/MPG 2.2-m telescope (Sec. 2.2). After fitting elliptical isophotes to the galaxy image we subtracted the model of each galaxy in the R-band to form a residual image and then we examined their isophotal shape parameters. The internal structure of 9 galaxies (excluding ESO153-G003) is explored using their residual images (Fig. 5) and the radial profile of their isophotal shape parameters (Fig. 6).

The galaxy ESO153-G003 is saturated in our images which prevents us detecting any internal fine structure and it shows no obvious extra tidal light. We briefly discuss the remaining 9 galaxies in turn. NGC 6653 shows a boxy structure in its outer part as revealed by a negative 4^{th} cosine term. NGC 6776 has probable dust within the central region of radius $\lesssim 3$ kpc ($8''$). It also reveals shell structures and extensive extra tidal light to the West and South. There is also a tidal tail extending in the southern direction. In both the B and R-bands, our images of NGC 6799 show a smooth elliptical profile and no morphological fine structure. NGC 6849 is disky in the outer part and there is some extra tidal light to the North. The 4^{th} cosine parameter shows negative values in the inner 4 kpc ($10''$) due to the effect of a foreground star located near the centre of the galaxy. Using multi-colour photometry, Saraiva, Ferrari & Pastoriza (1999) found that the isophotes in the B-band showed stronger variations in ellipticity, position angle and elliptical shape compared to the isophotes in the other bands. They suggested that NGC 6849 has traces of dust in the central part. Comparing the isophotal parameters for NGC 6849 from our B and R-band imaging, we find no evidence of such differences. NGC 7796 is a boxy galaxy reaching maximum boxiness in the inner region within a radius of 2 kpc ($10''$). MCG-01-03-018 shows traces of probable dust in central region. ESO107-G004 has a weak disky structure in the outer part at radii greater than 2 kpc ($10''$). ESO194-G021 shows a disk structure between 1 and 3 kpc ($5'' - 15''$). ESO462-

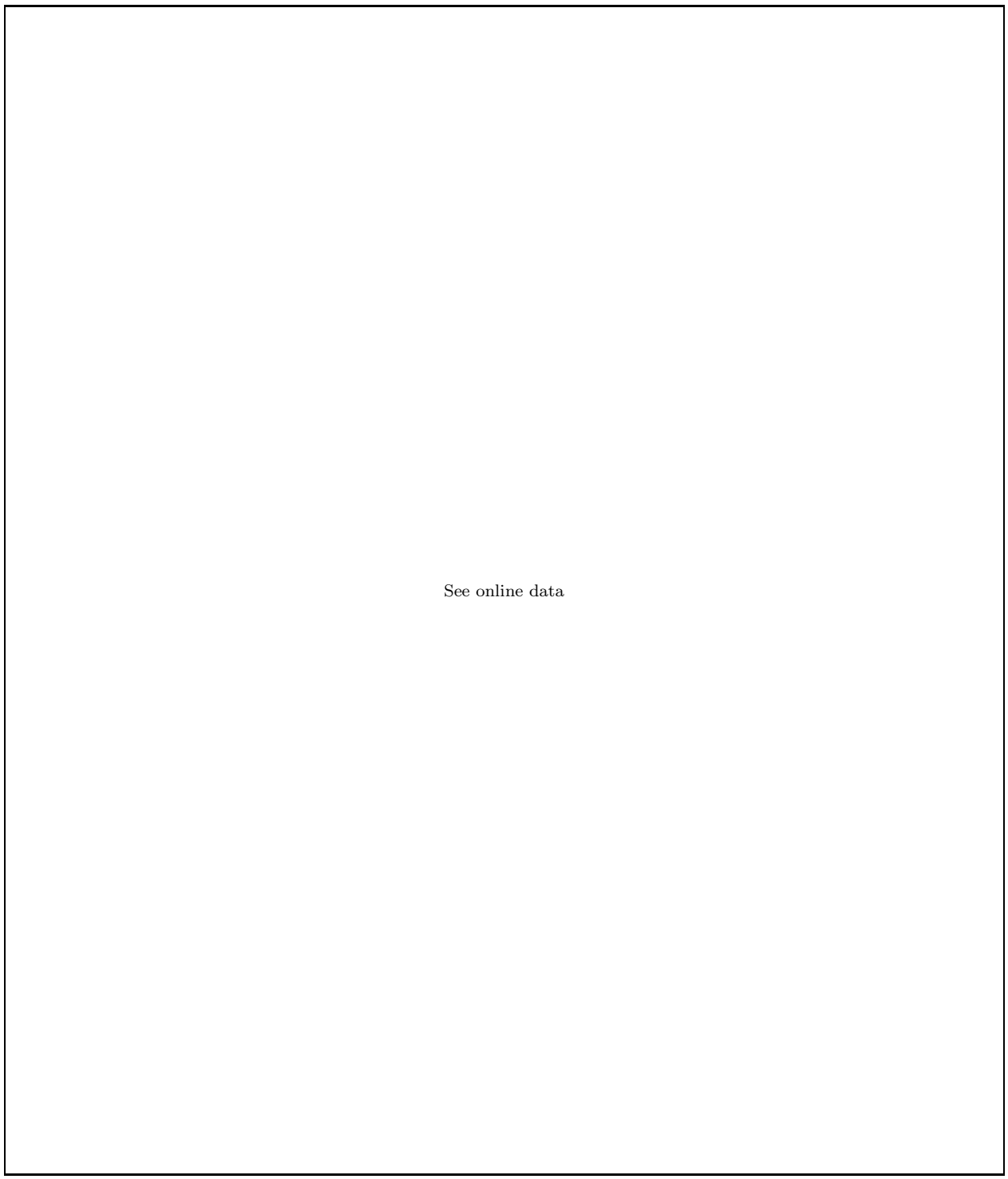

Figure 5. Residual images of galaxies in the R-band: NGC 6653, NGC 6776, NGC 6799, NGC 6849, NGC 7796, MCG-01-03-018, ESO107-G004, ESO194-G021 and ESO462-G015. Dust regions can be seen as bright features and extra light as dark features. All images have the same size of 188 × 155 sq. arcsec and oriented as North up and East to the left.

G015 shows a uniform elliptical structure of ellipticity ≈ 0.3 within a radius of 9 kpc ($25''$), but becomes disky at larger radii. Overall, 7 galaxies (out of 9) appear undisturbed with little or no fine structure.

4.3 The Fundamental Plane in $\log R_e$, $< \mu >_e$ and $\log \sigma$ space

JFK93 used their imaging observations in the Johnson B and Gunn r-bands, and the central velocity dispersion measurements from Faber et al. (1989) and Dressler (1987), for 33 early-type galaxies in the Coma cluster to compute the

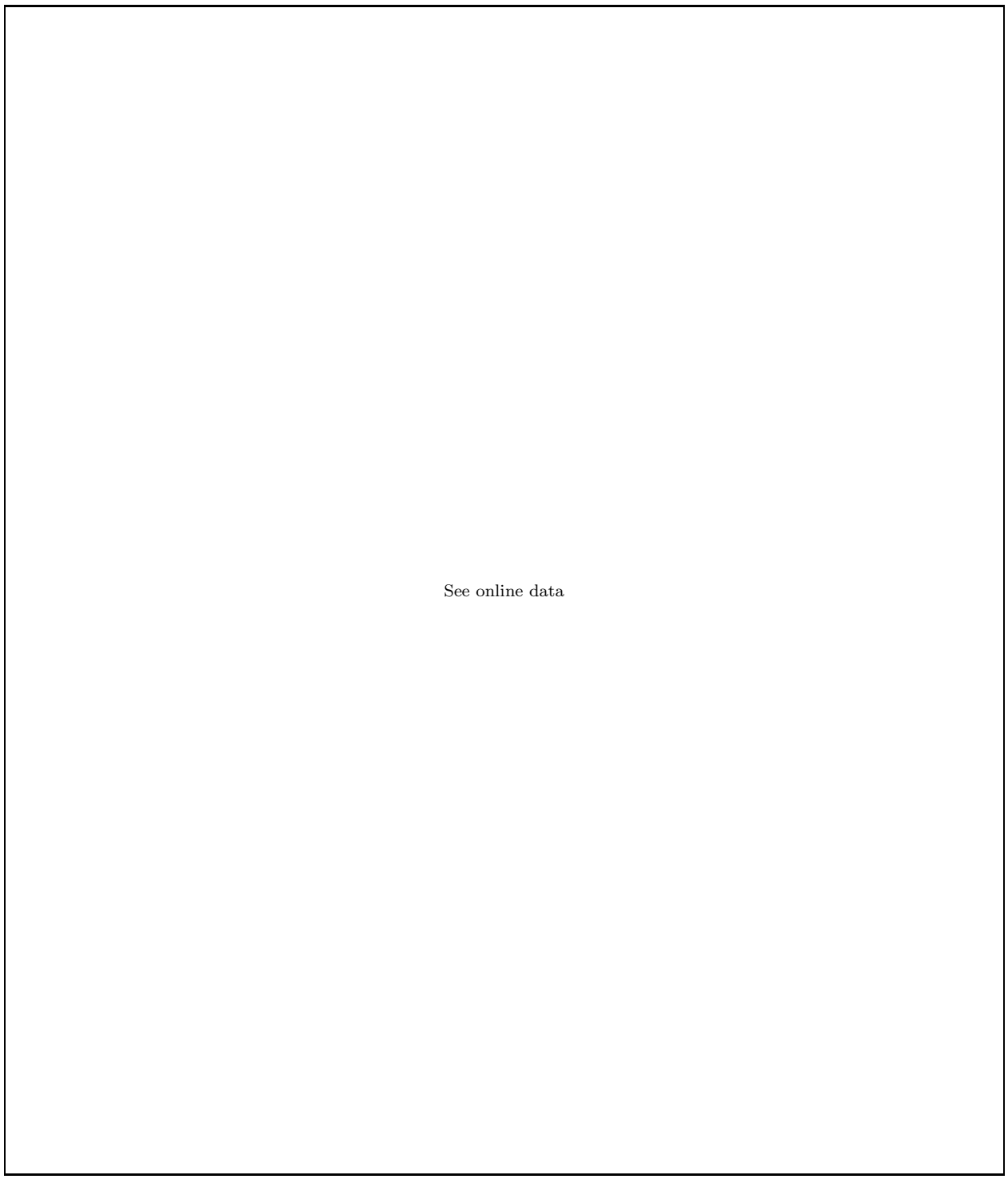

Figure 6. The R-band (open circles) surface brightness, ellipticity, position angle and 4^{th}-order cosine profiles. The upper panel for each galaxy shows also the B-band surface brightness (solid circles). The name of each galaxy is written above each set of four panels.

FP tilt and scatter. In the B-band, they found a FP of the form:

$$\log R_e = 1.203 \log \sigma + 0.352 < \mu >_e - 6.642 \quad (1)$$

where R_e values are in pc, and the intrinsic scatter is 0.027 dex. In Fig. 7, we show the edge-on projection of the FP for our isolated early-type galaxies using the parameters of JFK93. The solid line is the FP of the Coma cluster galaxies (Eq. 1). Considering a typical observational error in our data of 0.05, 0.1 and 0.05 in $\log R_e$, $< \mu >_B$ and $\log \sigma$ respectively and the intrinsic scatter of Coma galaxies, the 1σ scatter of the FP is shown in Fig. 7. Our galaxies show a similar tilt and scatter as the Coma cluster galaxies, except for the four galaxies NGC 2865, NGC 6172, NGC 6776 and NGC 6799 which deviate strongly from the FP. The 3 former galaxies

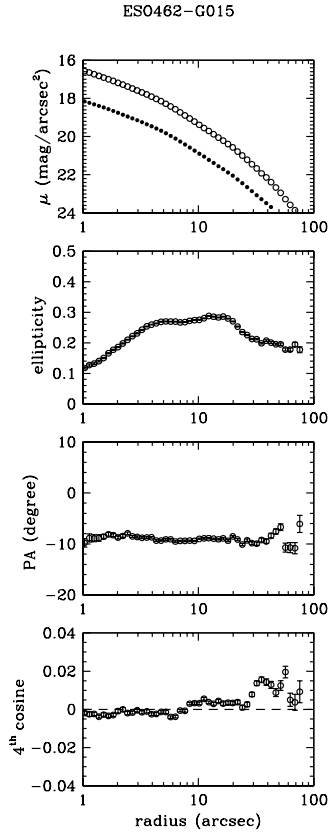

Figure 6 – *continued*

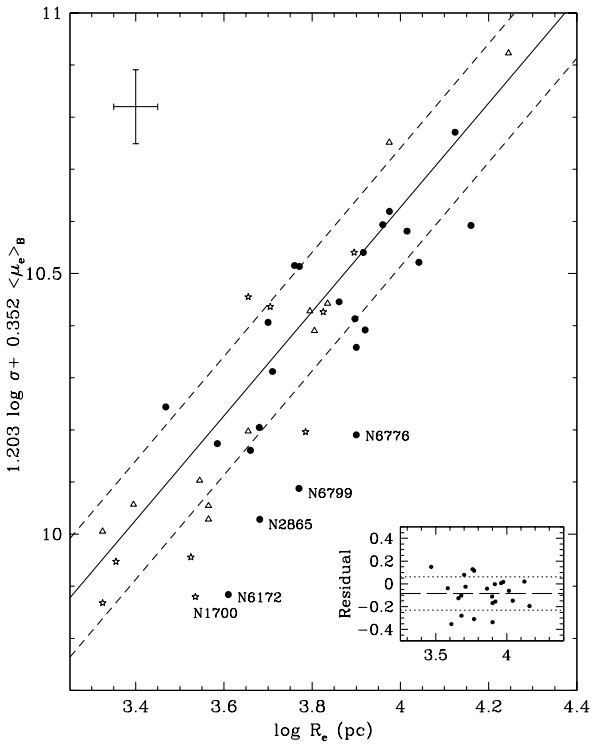

Figure 7. The edge-on view of the Fundamental Plane for the isolated galaxies in Table 2. The solid line is the Fundamental Plane of galaxies in Coma cluster from Jørgensen, Franx & Kjærgaard (1993). The short-dashed lines represent the 1σ dispersion of galaxies in Coma cluster from the same reference. Filled circles are our isolated galaxies in Table 2. Open triangles are galaxies in Hickson Compact Groups and stars are galaxies in the field or loose groups (de la Rosa et al. 2001). Galaxies NGC 2865, NGC 6172, NGC 6776 and NGC 6799 are the most deviant isolated galaxies from the FP and have young ages. The young loose group galaxy NGC 1700 also deviates from the FP. A typical error bar is shown. The inset shows the distribution of the residuals as in Fig. 1. The majority (15/23) of our isolated galaxies show negative residuals.

are 'young' galaxies of age less than 3.2 Gyrs (TF02; Denicoló et al. 2005b, D05b), while NGC 6799 has no published age. We note that such ages are luminosity-weighted central ages based on Lick absorption lines and single stellar population models to break the age-metallicity degeneracy. Such ages should not be considered absolute but rather relative ages. Several other caveats about the application of Lick-style ages to galaxy populations are discussed in Terlevich & Forbes (2002).

Considering the all 23 isolated galaxies in Fig. 7, their residuals from the FP of the Coma cluster show a mean offset of –0.08 and a 1σ dispersion of ~ 0.15 (see inset of Fig. 7). About two thirds (15/23) of our isolated galaxies show negative residuals.

From de la Rosa, de Carvalho & Zepf (2001), we take data for 12 elliptical galaxies in Hickson Compact Groups and 7 galaxies in the field or loose groups as a comparison sample. These galaxies cover the same range of R_e, $<\mu>_e$ and σ as our galaxies. We have excluded galaxies with spectra of S/N < 45. We also excluded NGC 4552 which was reported by Caon, Capaccioli & Rampazzo (1990) as a tidally distorted elliptical galaxy with an odd luminosity profile. We find that the sample of de la Rosa et al. also follows a FP similar to that of the Coma cluster ellipticals and the isolated galaxies (Fig. 7). The only exception is NGC 1700 which is also a young galaxy of age ≈ 2 Gyrs (TF02).

4.4 The Fundamental Plane in κ-space

By a simple orthogonal coordinate transformation (i.e., a rotation), Bender, Burstein & Faber (1992) introduced a different expression for the FP in terms of kappa (κ) space. The axes of this coordinate system are directly proportional to the galaxies physical parameters. The edge-on view of the FP is represented by κ_1 and κ_3, where κ_1 is a measure of the galaxy mass ($\log M$) and κ_3 is related to the M/L ratio.

In Fig. 8 we show the distribution of our isolated galaxies in the κ_1-κ_3 space. They show a similar tilt and dispersion to those of Virgo cluster galaxies from Bender et al. (1992). The 5 galaxies that show a strong deviation from the FP in Fig. 7, also show a tendency to have smaller κ_3 values i.e. smaller M/L ratio as expected for their young ages. The residuals of the isolated galaxies show a mean value of about –0.01 with 1σ dispersion of ~ 0.11 (see inset of Fig. 8) which indicates a good symmetry of our isolated galaxies about the FP of the Coma cluster in the κ space.

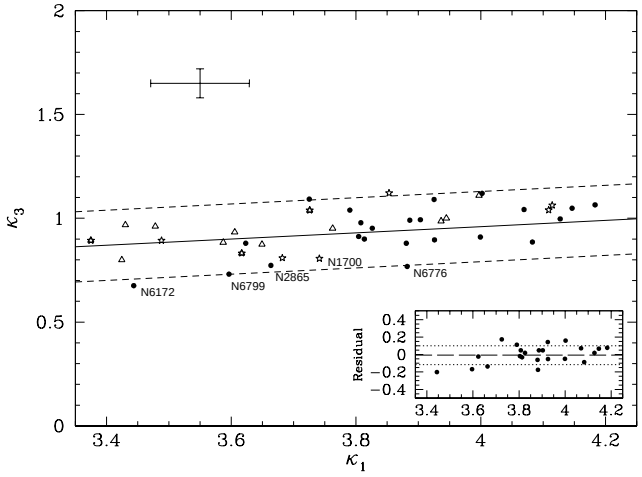

Figure 8. The edge-on view of the FP of the isolated galaxies in the κ_1-κ_3 space. Filled circles are our isolated sample. The solid line is the FP for Virgo cluster galaxies from Bender, Burstein & Faber (1992). The short-dashed lines represent the typical observational errors added to the 1σ intrinsic scatter of 0.05 in κ_3 for Virgo cluster galaxies (Nipoti, Londrillo & Ciotti 2003). Solid circles are the isolated galaxies. Open triangles are galaxies in Hickson Compact Groups and stars are galaxies in the field or loose groups (de la Rosa et al. 2001). The highly deviant galaxies from the FP in Fig. 7 show a tendency to have smaller κ_3 values than the average. A typical error bar is shown. The inset shows the distribution of the residuals as in Fig. 1

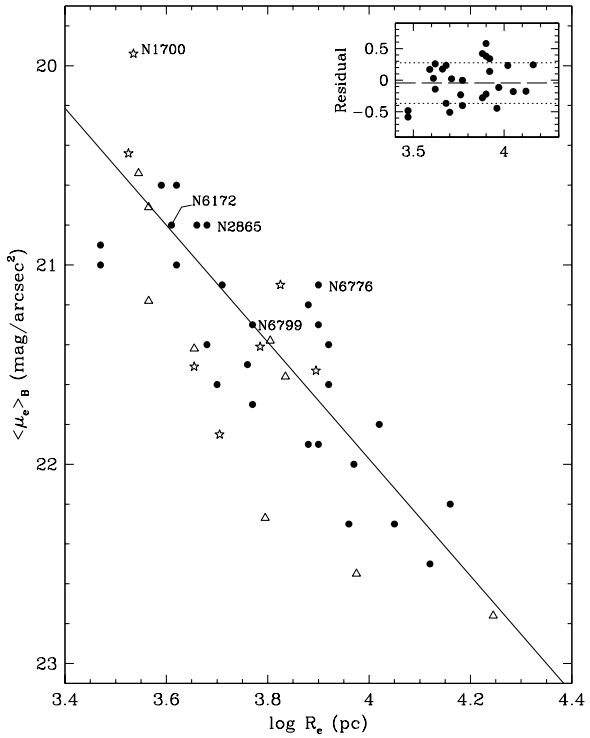

Figure 9. The projection of the FP in the plane of the mean surface brightness within the effective radius $< \mu_e >_B$ and effective radius R_e in the B. The solid line represents the Hamabe & Kormendy (1987) relation. The zero-point of the original relation has been shifted from V to the B-band assuming typical colours of $B-V=0.9$. Symbols as in Fig. 7. The inset shows the distribution of the residuals as in Fig. 1. Our isolated galaxies are generally consistent with the Hamabe & Kormendy relation for luminous galaxies.

4.5 The $< \mu_e >_B$-R_e relation

In Fig. 9, we show the projection of the FP in the plane of the mean surface brightness within the effective radius $< \mu_e >_B$ and effective radius R_e in the B-band. The solid line represents the Hamabe & Kormendy (1987) relation $\mu_e(V) = 2.94\log(\mathrm{R_e}) + 19.48$ shifted from V to the B-band assuming typical colours of $B-V=0.9$. We also transformed the surface brightness (μ_e) at R_e to $< \mu_e >$ using the relation of Graham & Colless (1997). Our isolated galaxies are generally consistent with the Hamabe & Kormendy relation for luminous galaxies. In the figure we also show the galaxies in the field and group sample of de la Rosa et al. (2001) which also show good consistency with the original relation. We note that, while the two galaxies NGC 6172 and NGC 6799 lie on the relation, the two isolated galaxies NGC 2865 and NGC 6776 and the group galaxy NGC 1700 show significant deviations.

In the inset in Fig. 9 we show the distribution of the residual of our isolated galaxies from the Hamabe & Kormendy relation. The mean values of the residuals show a slight negative offset of about –0.05 and 1σ dispersion of 0.32.

5 DISCUSSION

In this paper we have presented the CMR for 22 isolated early-type galaxies. We find that the isolated galaxies follow a similar CMR slope and scatter to that of galaxies in clusters. Theoretical studies of the CMR indicate that early-type galaxies formed the bulk of their stars at an early epoch of $z > 2$ (e.g. Bower, Lucey & Ellis 1992; Stanford, Eisenhardt & Dickinson 1995, 1998; Ellis et al. 1997; Bower, Kodama & Terlevich 1998; Bernardi et al. 2003c; Tantalo & Chiosi 2004). None of our isolated galaxies show the extremely blue colours seen in the isolated galaxy sample of Marcum, Aars & Fanilli (2004). On the other hand the isolated galaxy ESO194-G021 shows a very red colour of $B-R=1.73\pm0.14$ for its luminosity ($M_R=-21.5$).

Considering the morphological investigation of the 9 galaxies in Paper I and 9 galaxies in the present study, only two galaxies (11 per cent), NGC 2865 and NGC 6776, show obvious shell structures. This is less than the frequency found by Malin & Carter (1983), Seitzer & Schweizer (1990) and Reduzzi, Longhetti & Rampazzo (1996) who quoted higher fractions of 17, >50 and 16.4 per cent respectively for shell galaxies in low-density environments. On the other hand, we find more shells than Marcum et al. (2004) who detected no shells in any of their 8 isolated early-type galaxies. If evidence of a past merger includes shells, dust, plumes, disky and boxy structures, then we detected mergers in 60 per cent (11/18) of our isolated galaxies. This is a higher fraction than the 44 per cent quoted by Reduzzi et al. (1996) for their sample of 61 isolated early-type galaxies. Also, a recent study by Michard & Prugniel (2004) found

the frequency of galaxies with perturbed morphologies in poor group environments to be ≈ 35 per cent compared to only ≈ 19 per cent in the Virgo cluster. About 28 per cent (5/18) of our galaxies contain dust which is comparable to the 24.6 per cent of dusty galaxies quoted by Reduzzi et al. (1996). None of our 18 galaxies show irregular structure (radial changes between boxy and disky structures within the galaxy) compared to the 50 per cent found by Zepf & Whitmore (1993) for ellipticals in Hickson Compact Groups. We speculate that the high density of Hickson Compact Groups and the resultant high interaction rate gives rise to irregular isophotes whereas in isolated environments such interactions do not occur.

In Figures 7 and 8 we have compared the FP for our isolated early-type galaxy sample with that for galaxies in higher density environments. We find that galaxies in a wide range of environments are consistent with the same FP of similar tilt and scatter. In Fig. 7, the four galaxies NGC 2865, NGC 6172, NGC 6776 and NGC 6799 of our isolated sample and the group galaxy NGC 1700 of de la Rosa et al. (2001) deviate strongly from the main trend of the FP. In Fig. 8, the same five galaxies show a tendency to have smaller κ_3 in the direction of lower M/L ratios which can be explained by the young age of their stellar population.

We note that the isolated galaxies NGC 2865 and NGC 6776 and the group galaxy NGC 1700 also deviate from the $< \mu_e >_B$-R_e relation (Fig. 9). This indicates either a relatively large effective radius or high surface brightness. The isolated galaxies NGC 6172 and NGC 6799 lie on the Kormendy relation. The deviation of these two galaxies from the FP can be accounted for by their small velocity dispersions which are about 75 per cent of the expected values for their luminosities (Forbes & Ponman 1999).

The relative mean age of our galaxy sample can be estimated using the values quoted in TF02 and D05b. In their catalogues, the authors used Hβ and [MgFe] absorption line indices to break the age/metalicity degeneracy. These ages reflect the young stars in the central regions which were presumably formed during the last gaseous merger event. Therefore, the measured ages of these stellar populations give an estimate of the time elapsed since the last gaseous merger. Twelve galaxies (out of 23) of our sample have available published ages. The mean age of these galaxies is 4.6 $\pm$1.4 Gyr, which is approximately similar to the mean age quoted by Proctor et al. (2004) for galaxies in small groups and field (5.9 ± 0.7 Gyr) but younger than galaxies in cluster environments ($> 8.5 \pm 0.7$ Gyr).

In Fig. 7, we note that the most deviant galaxies from the FP are the 4 youngest galaxies of our sample with ages $\lesssim$ 3 Gyr. NGC 2865 has a relatively blue colour of $B - R = 1.3$ (Paper I) and reveals many fine structures such as shells, tidal light, dust and a kinematically distinct core (Paper I; Hau, Carter & Balcells 1999) which implies a past merger involving at least one gas-rich progenitor. Hau et al. (1999) quoted an age estimate of ~ 1.1 Gyr since the last merger which is comparable to the stellar population age of < 1.5 Gyr estimated by TF02. NGC 6776 has a tidal tail, shells and extensive extra tidal light. The tidal tail suggests at least one of the progenitors was a disk galaxy. In a detailed photometric and spectroscopic study of NGC 6776, Sansom, Reid & Boisson (1988) measured a rapid rotation of ≈ 100 km/s and a velocity dispersion of ≈ 200 km/s . They detected no dust or young stars which led them to conclude that the merger occurred $\geqslant 1$ Gyr ago. TF02 measured an age of 3.2 Gyr for its stellar population.

While the residual image of NGC 6172 (Paper I) did not reveal any obvious features, the unsharp-masking and colour map by Colbert, Mulchaey & Zabludoff (2001) revealed a weak shell and some dust near the centre of the galaxy. Its global blue colour ($B - R = 1.3$; Paper I) and the young age of 1.6 Gyr (D05b) suggest a recent starburst induced by a merger. NGC 6799 has a large dust lane along its eastern edge (Colbert et al. 2001). The residuals from the FP, using the method of PS96, is -0.37 which suggests the presence of a young stellar population of age $\lesssim 1.5$ Gyr (Forbes, Ponman & Brown 1998). This evidence supports the suggestion of a merger past for NGC 6799.

Despite the young age of 2.7 and 5.4 Gyr for NGC 1045 and ESO462-G015 respectively (D05b), and the tidal tail that was detected in NGC 1045 (Paper I) indicating a recent merger, they both lie within 1σ of the FP. The two galaxies NGC 6849 and MCG-01-03-018, have very old ages (TF02; D05b). The old age for their central stellar populations and the absence of fine structures suggests that there has not been a gaseous merger in the recent past for these two galaxies. The galaxy NGC 1132 reveals an extended group-like X-ray structure. This lead Mulchaey & Zabludoff (1999) to speculate that this galaxy was a remnant of a merged group of galaxies (a fossil). The absence of fine structure and an old central stellar population (D05b) suggests that it formed at early epochs and has not accreted any gas-rich galaxies recently.

Numerical simulations show that dissipational mergers between two disk, star-forming and gas-rich galaxies can produce non-homologous galaxies reproducing the observed tilt and scatter of the FP (Bekki 1998). Dissipationless mergers can also reproduce the FP (Hjorth & Madsen 1995; Capelato et al. 1995; Levine 1997; Dantas et al. 2003; Nipoti et al. 2003). However, as Nipoti et al. (2003) point out, dissipationless merging has difficulty explaining other scaling relations such as the colour-magnitude and black hole mass-σ relations. Unlike major mergers, neither accretion of smaller galaxies or a simple monolithic collapse are plausible scenarios to reproduce the FP (Dantas et al. 2003; Nipoti et al. 2003), however more realistic collapse conditions need to be explored.

6 SUMMARY AND CONCLUSION

In this paper we show that isolated early-type galaxies follow a colour-magnitude relation of similar slope and scatter to that of early-type galaxies in the dense environments of the Coma cluster. This would suggest that early-type galaxies formed the bulk of their stars at $z > 2$ (10.3 Gyrs ago in the ΛCDM cosmology). The scatter in this relation is explained as a result of a secondary starburst, resulting from a gaseous merger at a later epoch.

Two galaxies (11 per cent) of our isolated galaxies sample reveal shells. On the other hand, about 60 per cent (11/18) of our isolated galaxies revealed evidence of past mergers such as shells, dust, plumes, disky and boxy structures. Four of these eleven galaxies are the youngest members of our sample with ages $\lesssim 3$ Gyrs.

We also present the Fundamental Plane for our sample of isolated early-type galaxies. It shows a similar tilt and scatter to that for galaxies in denser environments. However some galaxies deviate from the relation due to the young age of their stellar populations or lower velocity dispersions. These young galaxies also show tendency to have smaller mass-to-light ratios in κ-space. The distribution of these galaxies in the $< \mu_e >_B$-R_e (Kormendy) projection is consistent with this interpretation.

Galaxies in such isolated environments show a relatively young mean age which is similar to that of galaxies in the field and small groups, but is younger than that for galaxies in clusters and Hickson Compact Groups. This result is qualitatively consistent with the expectations of the hierarchical galaxy formation.

From these results we conclude that relatively recent mergers offer a plausible explanation for the observed photometric and kinematic properties of *some* isolated early-type galaxies. For other isolated galaxies, which show neither fine structure or young stellar populations, we speculate that they formed at early epochs and evolved passively thereafter.

ACKNOWLEDGEMENTS

Thanks to Paul Goudfrooij and Vera Kozhurina-Platais for supplying us with the reduced images observed with the ESO/MPG telescope. We would also like to thank Ale Terlevich for his help with the observations. We wish to thank Dr. S. Brough for her useful comments in the final revision of this paper.

REFERENCES

Bekki K., 1998, ApJ, 496, 713
Bender R., Burstein D., Faber S. M., 1992, ApJ, 399, 462
Bernardi M. et al., 2003a, AJ, 125, 1849
Bernardi M. et al., 2003b, AJ, 125, 1866
Bernardi M. et al., 2003c, AJ, 125, 1882
Bower R. G., Lucey J. R., Ellis R. S., 1992, MNRAS, 254, 601
Bower R. G., Kodama T., Terlevich A., 1998, MNRAS, 299, 1193
Caon N., Capaccioli M., Rampazzo R., 1990, A&AS, 86, 429
Capelato H. V., de Carvalho R. R., Carlberg R. G., 1995, ApJ, 451, 525
Colbert J.W., Mulchaey J.S., Zabludoff A.I., 2001, AJ, 121, 808
Dantas C. C., Capelato H. V., Ribeiro A. L. B., de Carvalho R. R., 2003, MNRAS, 340, 398
de Carvalho R. R., Djorgovski S., 1992, ApJ, 389, 49
de la Rosa I. G., de Carvalho R. R., Zepf S. E., 2001, AJ, 122, 93
Denicoló G, Terlevich R, Terlevich E., Forbes D. A., Terlevich A., Carrasco L., 2005a, MNRAS, 356, 1440 (D05a)
Denicoló G, Terlevich R, Terlevich E., Forbes D.A., Terlevich A., 2005b, MNRAS, 358, 813 (D05b)
Djorgovski S., Davis M., 1987, ApJ, 313, 59
Djorgovski S., de Carvalho R., Han M. S. , 1988, in Pritchet C. J., van der Bergh S., eds, ASP Conf. Ser. Vol. 4, The Extragalactic Distance Scale. Astron. Soc. Pac., San Francisco, p. 329
Dressler A., 1987, ApJ, 317, 1
Ellis R.S., Smail I., Dressler A., Couch W.J., Oemler A., Butcher H., Sharples, R.M., 1997, ApJ, 483, 582
Evstigneeva E.A., Reshetnikov V.P., Sotnikova N. Ya., 2002, A&A, 381, 6
Faber S.M., Wegner G., Burstein D., Davies R.L., Dressler A., Lynden-Bell D., Terlevich R.J., 1989, ApJS, 69, 763
Forbes D.A., Ponman T., 1999, MNRAS, 309, 623
Forbes D.A., Ponman T.J., Brown R.J.N., 1998, ApJ, 508, 43
Gladders M.D., Lopez-Cruz O., Yee H.K.C., Kodama T., 1998, ApJ, 501, 571
Graham A., Colless M., 1997, MNRAS, 287, 221
Hamabe M., Kormendy J., 1987, in de Zeeuw T., ed., Proc. IAU Symp. 127, Structure and Dynamics of Elliptical Galaxies. Reidel, Dordrecht, p. 379
Hau G.K.T., Carter D., Balcells M., 1999, MNRAS, 306, 437
Hau G.K.T., Forbes D.A., 2005, in preparation (HF05)
Hjorth J., Madsen J., 1995, ApJ, 445, 55
Jørgensen I., Franx M., Kjærgaard P., 1993, ApJ, 411, 34 (JFK93)
Jørgensen I., Franx M., Kjærgaard P., 1995, MNRAS, 276, 1341 (JFK95)
Kauffmann G., White S.D. M., Heckman T.M., Mnard B., Brinchmann J., Charlot S., Tremonti C., Brinkmann J., 2004, MNRAS, 353, 713
Koprolin W., Zeilinger W.W., 2000, A&AS, 145, 71
Landolt A. U., 1992, AJ, 104, 340
Levine S., 1997, The Nature of Elliptical Galaxies; 2nd Stromlo Symposium. ASP Conference Series; Vol. 116; 1997; ed. Arnaboldi M., Da Costa G.S. and Saha P., p.166
Malin D.F., Carter D., 1983, ApJ, 274, 534
Marcum P. M., Aars C. E., Fanelli M. N., 2004, AJ, 127, 3213
Michard R., Prugniel P., 2004, A&A, 423, 833
Mulchaey J.S., Zabludoff A.I., 1999, ApJ, 514, 133
Nipoti C., Londrillo P., Ciotti L., 2003, MNRAS, 342, 501
Proctor R. N., Forbes D. A., Hau G. K. T., Beasley M. A., De Silva G. M., Contreras R., Terlevich A. I., 2004, MNRAS, 349, 1381
Prugniel Ph., Heraudeau Ph., 1998, A&ASS, 128, 299 (PH98)
Prugniel Ph., Simien F., 1996, A&A, 309, 749 (PS96)
Reda F.M., Forbes D.A., Beasley M., O'Sullivan E.J., Goudfrooij P., 2004, MNRAS, 354, 851 (Paper I)
Reduzzi L., Longhetti M., Rampazzo R., 1996, MNRAS, 282, 149
Sansom A. E., Reid I. Neill, Boisson C., 1988, MNRAS, 234, 247
Saraiva M.F., Ferrari F., Pastoriza M.G., 1999, A&A 350, 399
Schlegel D.J., Finkbeiner D.P., Davis M., 1998, ApJ, 500, 525
Seitzer P., Schweizer F., 1990, Dynamics and Interactions of Galaxies, ed. R. Weilen (New York: Springer), 270
Stanford S.A., Eisenhardt P.R.M., Dickinson M.E., 1995, ApJ, 450, 512
Stanford S.A., Eisenhardt P.R.M., Dickinson M.E., 1998, ApJ, 492, 461
Tantalo R., Chiosi C., 2004, MNRAS, 353, 405
Terlevich A.I., Forbes D.A., 2002, MNRAS, 330, 547 (TF02)
Trujillo I., Burkert A., Bell E.F., 2004, ApJ, 600, 39
Zepf S.E., Whitmore B.C., 1993, ApJ, 418, 72

This figure "fig5.jpg" is available in "jpg" format from:

http://arXiv.org/ps/astro-ph/0505265v1

This figure "fig6.jpg" is available in "jpg" format from:

http://arXiv.org/ps/astro-ph/0505265v1